Figure S1. Related to Figure 1.

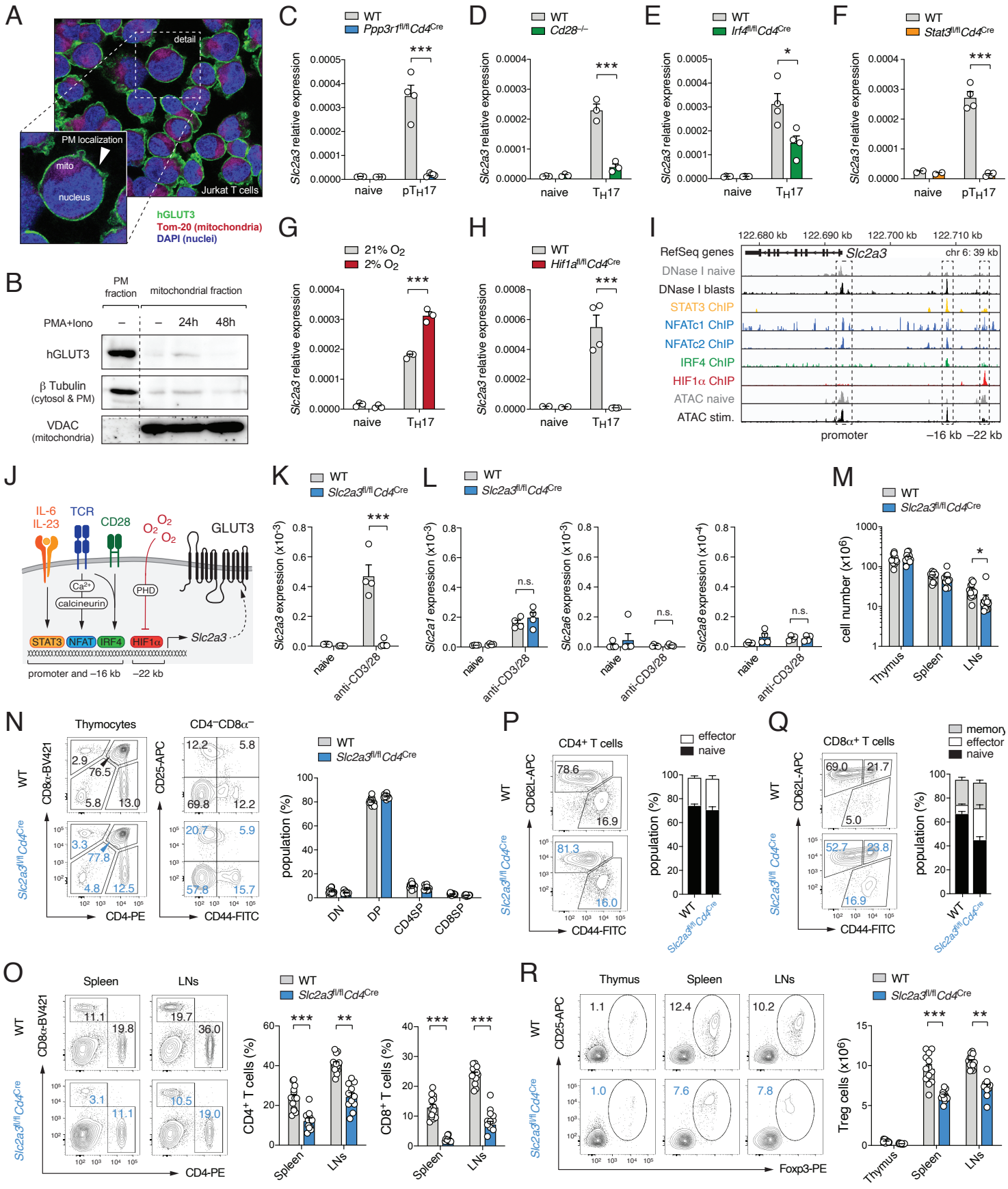

Figure S1. GLUT3 expression in Th17 cells and the phenotype of mice with T cell-specific ablation of GLUT3 (related to Fig. 1)**. (A and B)** Analysis of subcellular GLUT3 expression in Jurkat T cells using immunofluorescence **(A)** or immunoblot **(B)** analyses. **(C-J)** GLUT3 expression in Th17 cells is coordinated by multiple pathways. **(C)** *Slc2a3* (GLUT3) gene expression in naïve and differentiated Th17 cells of WT and *Ppp3r1*$^{fl/fl}$*Cd4*^{Cre} mice with conditional deletion of the calcineurin regulatory subunit Bα in T cells; means ± SEM of 4 mice. **(D)** *Slc2a3* (GLUT3) gene expression in naïve and differentiated Th17 cells of WT and CD28-deficient (*Cd28*$^{-/-}$) mice; means ± SEM of 3 mice. **(E)** Analysis of *Slc2a3* (GLUT3) gene expression in naïve and differentiated Th17 cells of WT and *Irf4*$^{fl/fl}$*Cd4*^{Cre} mice with conditional deletion of IRF4 in T cells; means ± SEM of 4 mice. **(F)** *Slc2a3* (GLUT3) gene expression analysis in naïve and differentiated Th17 cells of WT and *Stat3*$^{fl/fl}$*Cd4*^{Cre} mice with conditional deletion of STAT3 in T cells; means ± SEM of 4 mice. **(G)** Analysis of *Slc2a3* (GLUT3) gene expression Th17 cells differentiated under normoxic (21% O_2) and hypoxic (2% O_2) culture conditions for 3 days; means ± SEM of 3 mice. **(H)** *Slc2a3* (GLUT3) gene expression analysis in naïve and differentiated Th17 cells of WT and *Hif1a*$^{fl/fl}$*Cd4*^{Cre} mice with conditional deletion of HIF-1a in T cells; means ± SEM of 4 mice. **(I)** *In silico* analysis of the *Slc2a3* (GLUT3) gene locus in murine T cells. Chromatin accessibility was determined by genome-wide DNase I hypersensitivity analysis (Bevington *et al.*, 2016) and ATAC-seq. (Mognol *et al.*, 2017). Analysis of ChIP-seq datasets showed the binding of NFATc1 (Klein-Hessling *et al*. 2017) and NFATc2 (Martinez *et al.*, 2015) to the promoter region and to an –16 kb upstream regulatory element, binding of STAT3 (Hirahara *et al.*, 2015) and IRF4 (Man *et al.*, 2013) to the –16 kb element, and binding of HIF-1α (Ciofani *et al.*, 2012) to an additional element located –22 kb upstream of the *Slc2a3* transcription start site (TSS). **(J)** Upregulation of GLUT3 expression by antigen receptor ligation (TCR), co-stimulation (CD28) and cytokine signaling (IL-6/IL-23) is orchestrated by NFAT, IRF4, STAT3 and HIF-1 α in Th17 cells. **(K-R)** Analysis of mice with T cell-specific deletion of GLUT3 (*Slc2a3*$^{fl/fl}$*Cd4*^{Cre} mice). **(K** and **L)** Analysis of *Slc2a3* (GLUT3) **(K)**, *Slc2a1* (GLUT1), *Slc2a6* (GLUT6) and *Slc2a8* (GLUT8) **(L)** gene expression in naïve and anti-CD3/CD28 stimulated CD4$^+$ T cells of WT and *Slc2a3*$^{fl/fl}$*Cd4*^{Cre} mice by qRT-PCR; means ± SEM of 4 mice. **(M)** Total cell numbers of thymus, spleen and lymph nodes (LNs) of 8-14 weeks old WT and *Slc2a3*$^{fl/fl}$*Cd4*^{Cre} mice; means ± SEM of 11-13 mice. **(N)** Thymic development of T cells in WT and *Slc2a3*$^{fl/fl}$*Cd4*^{Cre} mice. Representative flow cytometric analyses of CD4$^-$CD8$^-$ (DN), CD4$^+$CD8$^+$ (DP) and single positive (SP) thymocytes of WT and *Slc2a3*$^{fl/fl}$*Cd4*^{Cre} mice; means ± SEM of 11-13 mice. **(O)** Analysis of peripheral T cell subsets in WT and *Slc2a3*$^{fl/fl}$*Cd4*^{Cre} mice. Representative flow cytometric analyses of CD4$^+$ and CD8$^+$ T cells in spleen and LNs of WT and *Slc2a3*$^{fl/fl}$*Cd4*^{Cre} mice; means ± SEM of 11-13 mice. **(P** and **Q)** Analysis of CD44$^-$CD62L$^+$ (naïve), CD44$^+$CD62L$^+$ (central memory) and CD44$^+$CD62L$^-$ (effector) CD4$^+$ **(P)** and CD8$^+$ **(Q)** T cells of WT and *Slc2a3*$^{fl/fl}$*Cd4*^{Cre} mice by flow cytometry; means ± SEM of 12-13 mice. **(R)** Analysis of Foxp3$^+$ Treg cell frequency and total cell number in the thymus, spleen and LNs of WT and *Slc2a3*$^{fl/fl}$*Cd4*^{Cre} mice; means ± SEM of 11-13 mice. Statistical analyses in (C-H), (K-M), (O) and (R) by unpaired Student's t-tests. *, p<0.05; **, p<0.01, ***, p<0.001.

Figure S2. Related to Figure 1.

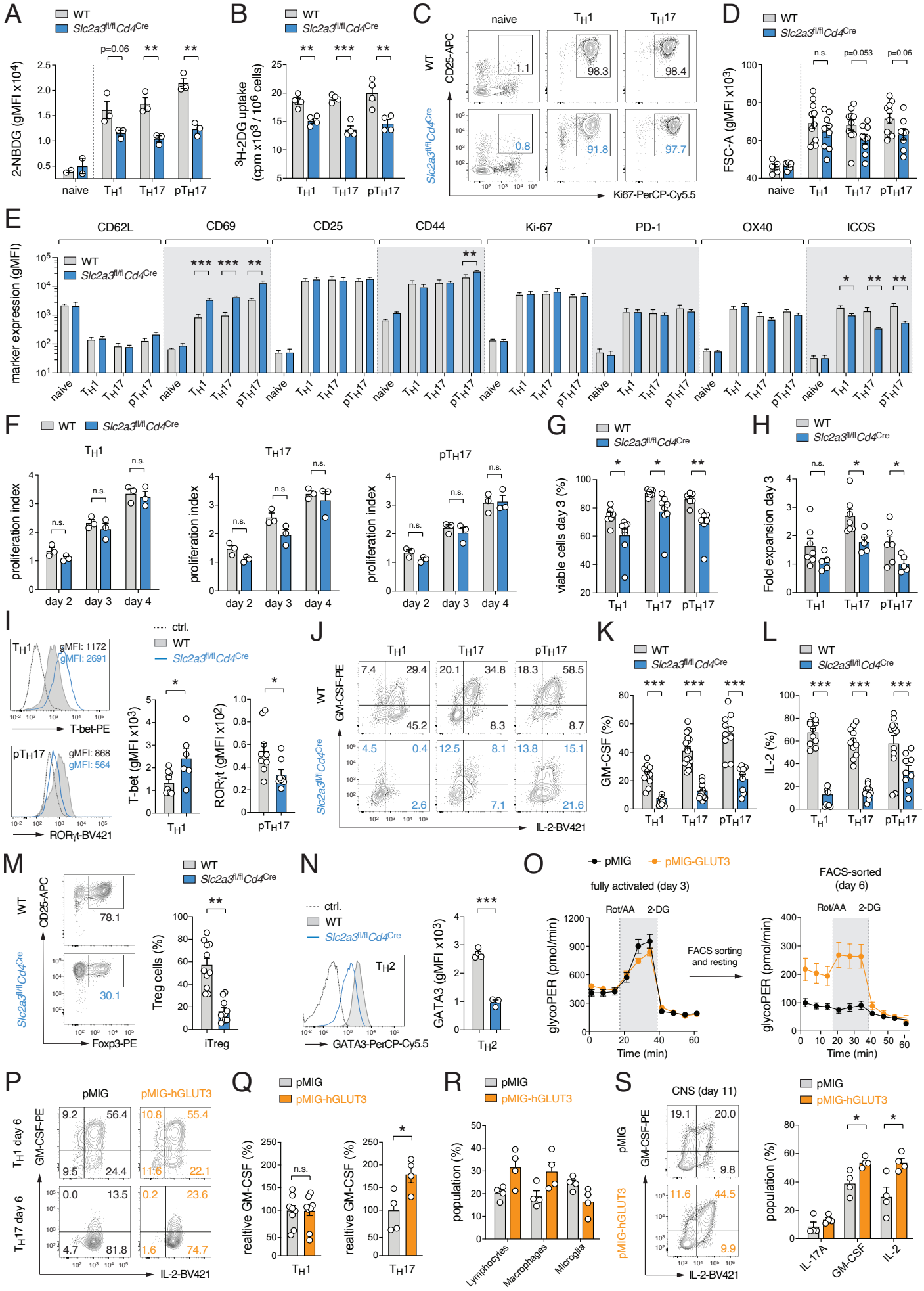

Figure S2. GLUT3-deficient T cells show normal activation and proliferation but defective Th17 cell effector function (related to Fig. 1)**. (A** and **B)** Analysis of glucose uptake by WT and GLUT3-deficient (*Slc2a3*$^{fl/fl}$*Cd4*^{Cre}) Th1 and Th17 cells using the fluorescent glucose analogue 2-NBDG **(A)** and tritiated [^{3}H] 2-desoxy-glucose (2-DG) **(B)**; means ± SEM of 2-4 mice. **(C** and **D)** Flow cytometric analysis of cell cycle entry (expression of CD25 and Ki-67) **(C)** and cell size (FSC-A) **(D)** of WT and GLUT3-deficient T cells after polarization for 3 days under Th1 and Th17 culture conditions. **(E)** Analysis of activation marker (CD69, CD25, CD44, Ki-67, PD-1, OX40, ICOS, CD62L) expression on WT and GLUT3-deficient T cells cultured for 3 days under Th1, Th17 and pTh17 culture conditions by flow cytometry; means ± SEM of 3-4 mice. **(F)** Proliferation analysis of WT and GLUT3-deficient Th1, Th17 and pTh17 cells by CFSE dilution over a course of 4 days *in vitro*; means ± SEM of 3 mice. **(G** and **H)** Analysis of viability **(G)** and cellular expansion **(H)** of WT and GLUT3-deficient T cells cultured for 3 days under Th1, Th17 and pTh17 culture conditions by flow cytometry; means ± SEM of 5-7 mice. **(I)** Flow cytometric analyses of T-bet and RORγt expression in WT and GLUT3-deficient T cells cultured for 3 days under Th1 and pTh17 cell-polarizing conditions; means ± SEM of 6-10 mice. **(J-L)** Flow cytometric analysis of GM-CSF **(K)** and IL-2 **(L)** production by WT and GLUT3-deficient Th1, Th17 and pathogenic Th17 (pTh17) cells after re-stimulation with PMA/Iono for 5 h; means ± SEM of 8-17 mice. **(M** and **N)** Analysis of Foxp3 **(M)** and GATA3 **(N)** expression in WT and GLUT3-deficient T cells differentiated under iTreg and Th2-polarizing conditions, respectively; means ± SEM of 3-11 mice. **(O-S)** Ectopic expression of GLUT3 in T cells augments the pathogenicity of Th17 cells. **(O)** Measurement of glycolytic proton efflux rate (PER) of GLUT3 or empty vector (EV)-transduced and FACS-sorted Th17 cells on day 3 and 6 of culture using a Seahorse extracellular flux analyzer; means ± SEM of 3 experiments. **(P** and **Q)** Flow cytometric analysis of GM-CSF and IL-2 cytokine production of GLUT3 and EV-transduced Th1 and Th17 after re-stimulation with PMA/Iono for 5 h; means ± SEM of 4-8 mice. **(R** and **S)** Ectopic expression of GLUT3 augments EAE immunopathology. **(R)** Analysis of immune cell populations in the CNS after transfer of EV or GLUT3-transduced 2D2 Th17 cells. **(S)** Analysis of IL-17, GM-CSF and IL-2 expression in CNS-infiltrating 2D2 T cells transduced with GLUT3 or EV; means ± SEM of 4 mice per cohort. Statistical analyses in (A), (B), (D-I), (K-N), (Q) and (S) by unpaired Student's t-tests. *, $p<0.05$, **, $p<0.01$, ***, $p<0.001$, n.s., non-significant.

Figure S3. Related to Figure 2.

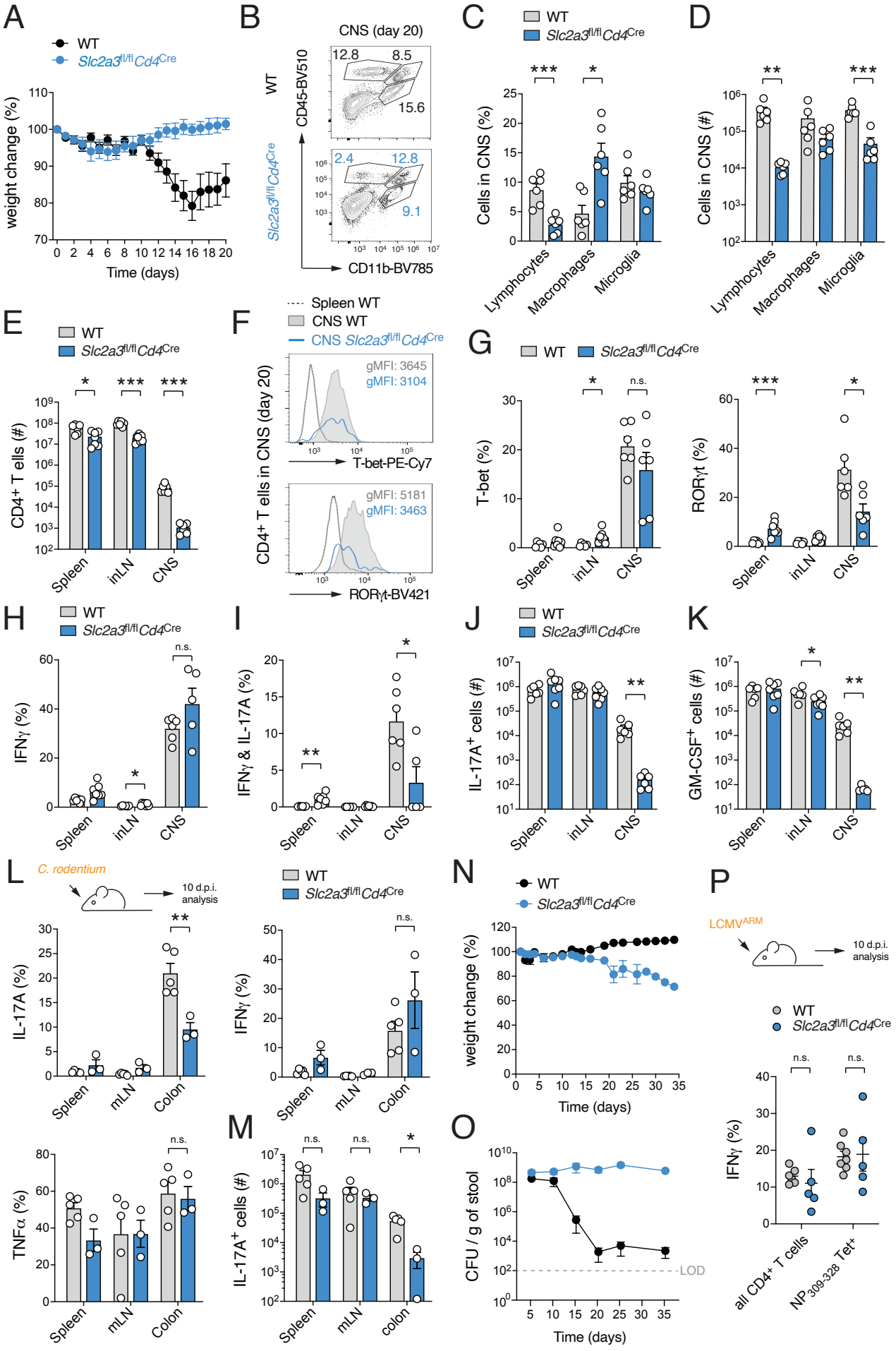

Figure S3. GLUT3 controls Th17 cell-mediated immunity *in vivo* (related to Fig. 2)**. (A**-**K)** T cell-specific GLUT3 deletion protects mice from experimental autoimmune encephalomyelitis (EAE). **(A)** Relative weight change of WT and *Slc2a3*$^{fl/fl}$*Cd4*^{Cre} mice after immunization with MOG_{35-55} peptide emulsified in CFA; means ± SEM of 9 mice per cohort. **(B**-**D)** Flow cytometric analysis of relative **(B** and **C)** and absolute numbers **(D)** of immune cell populations in the CNS of WT and *Slc2a3*$^{fl/fl}$*Cd4*^{Cre} mice after immunization with MOG_{35-55} peptide; means ± SEM of 6 mice per cohort. **(E)** Absolute $CD4^+$ T cell numbers in the spleen, inguinal lymph nodes (inLN) and CNS of WT and *Slc2a3*$^{fl/fl}$*Cd4*^{Cre} mice after immunization with MOG_{35-55} peptide; means ± SEM of 6 mice per cohort. **(F** and **G)** T-bet and RORγt transcription factor expression in encephalitic $CD4^+$ T cells in the spleen, inLNs and CNS of WT and *Slc2a3*$^{fl/fl}$*Cd4*^{Cre} mice after immunization with MOG_{35-55} peptide; means ± SEM of 6 mice per cohort. **(H**-**K)** Cytokine production of encephalitic $CD4^+$ T cells. Frequencies of IFNγ **(H)** and IFNγ plus IL-17 **(I)** as well as total cell numbers of IL-17 **(J)** and GM-CSF-producing **(K)** $CD4^+$ T cells in the spleen, inLNs and CNS of WT and *Slc2a3*$^{fl/fl}$*Cd4*^{Cre} mice 20 days after MOG_{35-55} immunization; means ± SEM of 5-7 mice. **(L**-**P)** GLUT3 controls Th17 cell effector function in response to *C. rodentium* infection. **(L)** Frequencies of IL-17, IFNγ and TNFα-producing T cells in the spleen, mesenteric (m)LNs and colon of WT and *Slc2a3*$^{fl/fl}$*Cd4*^{Cre} mice 10 days after *C. rodentium* infection; means ± SEM of 3-5 mice. **(M)** Absolute cell numbers of IL-17-producing $CD4^+$ T cells in the spleen, mLNs and colon of WT and *Slc2a3*$^{fl/fl}$*Cd4*^{Cre} mice 10 days after *C. rodentium* infection; means ± SEM of 3-5 mice. **(N** and **O)** Relative weight change **(N)** and bacterial load in the feces **(O)** of WT and *Slc2a3*$^{fl/fl}$*Cd4*^{Cre} mice after infection with *C. rodentium*; means ± SEM of 3-10 mice per cohort. (**P)** Analysis of IFNγ expression of all and LCMV-specific ($NP_{309-328}$ tetramer$^+$) $CD4^+$ T cells in the spleen of WT and *Slc2a3*$^{fl/fl}$*Cd4*^{Cre} mice 10 days after the infection with the Armstrong strain of LCMV; means ± SEM of 5-7 mice. Statistical analyses in (C-E), (G-M) and (P) by unpaired Student's t-tests. *, $p<0.05$, **, $p<0.01$, ***, $p<0.001$, n.s., non-significant.

Figure S4. Related to Figure 4.

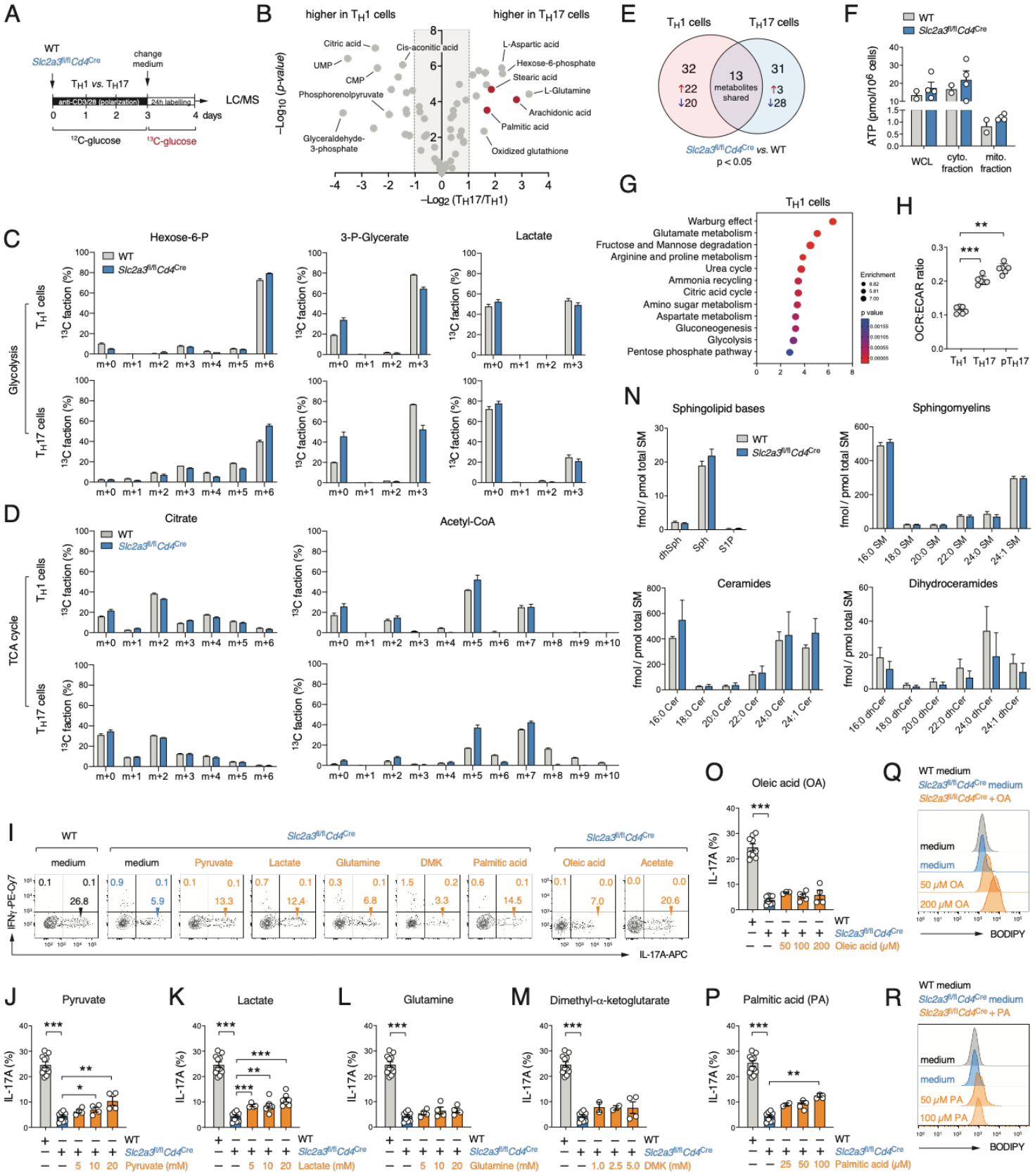

Figure S4. Tracing of glucose-derived metabolites in GLUT3-deficient Th1 and Th17 cells (related to Fig. 4)**. (A)** Experimental setup to trace ^{13}C-glucose-derived polar metabolites in WT and GLUT3-deficient (*Slc2a3*$^{fl/fl}$*Cd4*^{Cre}) Th1 and Th17 cells. **(B)** Volcano plot of differential metabolite concentrations between Th1 and Th17 cells, analysis is based on 4 biological replicates per T cell subset and genotype. **(C** and **D)** Metabolic tracing of glucose-derived ^{13}C-metabolites of the glycolytic pathway **(C)** and the tricarboxylic acid (TCA) cycle **(D)** in WT and GLUT3-deficient Th1 and Th17 cells; means ± SEM of 4 biological replicates. **(E)** Venn diagram analysis of > 2-fold differential metabolite concentrations ($p < 0.05$) comparing WT and GLUT3-deficient Th1 with Th17 cells; red and blue arrows indicate higher and lower metabolite abundances, respectively. **(F)** Analysis of ATP concentrations in whole cell lysates (WCL) and isolated cytosolic and mitochondrial fractions of WT and GLUT3-deficient Th17 cells; means ± SEM of 2-4 mice. **(G)** Metabolite set enrichment analysis (MSEA) of differential metabolite concentrations ($p < 0.05$) between WT and GLUT3-deficient Th1 cells. **(H)** Ratio of oxygen consumption rate (OCR) to extracellular acidification rate (ECAR) in Th1, Th17 and pathogenic (p)Th17 cells; means ± SEM of 6 experiments. **(I-M)** Effects of exogenous pyruvate **(J)**, lactate **(K)**, glutamine **(L)** and dimethyl-α-ketoglutarate **(M)** on the cytokine production of GLUT3-deficient Th17 cells. Flow cytometric analyses of IL-17 production of WT and *Slc2a3*$^{fl/fl}$*Cd4*^{Cre} Th17 cells treated with different metabolites for 24 h before re-stimulation with PMA/Iono; means ± SEM of 2- 11 mice. **(N-R)** Defective cytokine production is not due to impaired lipid metabolism in GLUT3- deficient Th17 cells. **(N)** Lipidomic analyses of sphingoid long-chain bases (dhSph, dihydrosphingosine; Sph, sphingosine; S1P, sphingosine 1-phosphate), sphingomyelins (SM), ceramides (Cer) and dihydroceramides (dhCer) in WT and GLUT3-deficient Th17 cells by LC/MS; means ± SEM of 3 mice. Effect of oleic **(O)** or palmitic acid **(P)** on the cytokine production of GLUT3-deficient Th17. Flow cytometric analyses of IL-17 production of WT and *Slc2a3*$^{fl/fl}$*Cd4*^{Cre} Th17 cells treated with oleic or palmitic acid for 24 h before re-stimulation with PMA/Iono for 5 h; means ± SEM of 2-11 mice. Neutral lipid content of WT and GLUT3-deficient Th17 cells after exogenous addition of oleic acid **(Q)** or palmitic acid **(R)** by flow cytometry using BODIPY labeling. Statistical analyses in (H), (J-M), (O) and (P) by unpaired Student's t-tests. **, $p<0.01$; ***, $p<0.001$.

Figure S5. Related to Figure 5

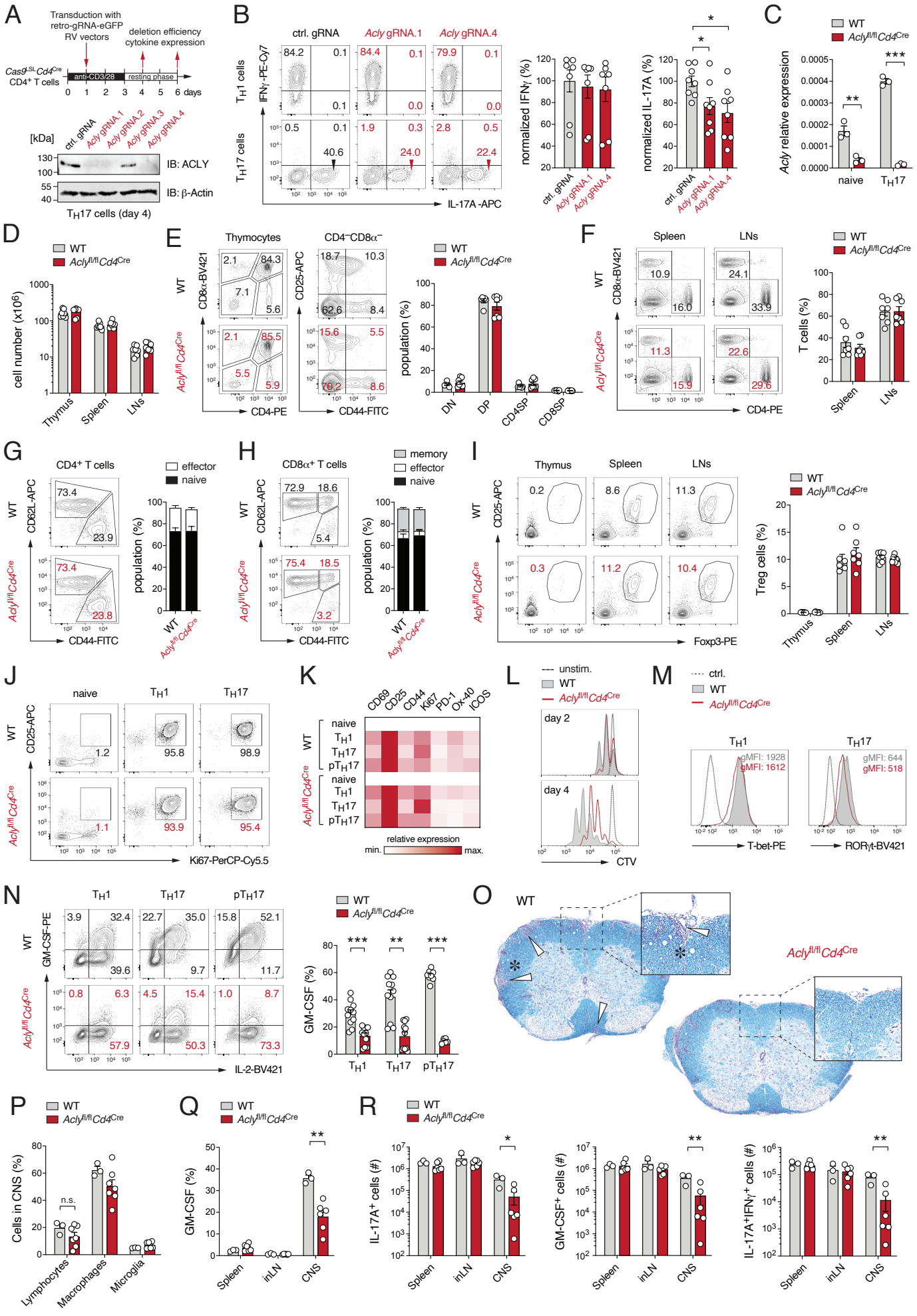

Figure S5. ACLY controls cytokine expression of Th17 cells (related to Fig. 5)**. (A** and **B)** Inducible deletion of ACLY in Th17 cells using CRISPR/Cas9-mediated gene editing. **(A)** Transduction of Cas9-expressing Th17 cells (isolated from *Rosa26*$^{LSL\text{-}Cas9}$*Cd4*^{Cre} mice) with retroviral vectors expressing control (ctrl.) or *Acly*-targeting gRNAs. Immunoblot analysis to confirm successful ACLY protein deletion 3 days after retroviral transduction. **(B)** Flow cytometric analysis of IFNγ and IL-17 production in Th1 and Th17 cells after Cas9-mediated ACLY deletion and stimulation with PMA/Iono for 5 h; means ± SEM of 8 mice. **(C)** Analysis of *Acly* gene expression in naïve and anti-CD3/CD28 activated WT and ACLY-deficient (*Acly*$^{fl/fl}$*Cd4*^{Cre}) CD4$^+$ T cells by qRT-PCR; means ± SEM of 3 mice. **(D-I)** Phenotypic characterization of lymphocyte subsets in WT and *Acly*$^{fl/fl}$*Cd4*^{Cre} mice. **(D)** Total cell number of thymus, spleen and lymph nodes (LNs) in 7-12 weeks old WT and *Acly*$^{fl/fl}$*Cd4*^{Cre} mice; means ± SEM of 7 mice. **(E)** Thymic development of T cells in WT and *Acly*$^{fl/fl}$*Cd4*^{Cre} mice. Representative flow cytometric analyses of CD4$^-$CD8$^-$ (DN), CD4$^+$CD8$^+$ (DP) and single positive (SP) thymocytes of WT and *Acly*$^{fl/fl}$*Cd4*^{Cre} mice and summary of 7 mice; means ± SEM. **(F)** Analysis of peripheral T cell subsets in WT and *Acly*$^{fl/fl}$*Cd4*^{Cre} mice; means ± SEM. **(G** and **H)** Analysis of CD44$^-$CD62L$^+$ (naïve), CD44$^+$CD62L$^+$ (central memory) and CD44$^+$CD62L$^-$ (effector) CD4$^+$ **(G)** and CD8$^+$ **(H)** T cells of WT and *Acly*$^{fl/fl}$*Cd4*^{Cre} mice by flow cytometry; means ± SEM of 7 mice. **(I)** Flow cytometric analysis of Foxp3$^+$ Treg cells in the thymus, spleen and LNs of WT and *Acly*$^{fl/fl}$*Cd4*^{Cre} mice; means ± SEM of 7 mice. **(J)** Analysis of cell cycle entry (expression of CD25 and Ki-67) of WT and ACLY-deficient CD4$^+$ T cells after polarization for 3 days under Th1 and Th17 culture conditions. **(K)** Activation marker expression (CD69, CD25, CD44, Ki-67, PD-1, OX40, ICOS) on WT and ACLY-deficient (*Acly*$^{fl/fl}$*Cd4*^{Cre}) T cells cultured for 3 days under Th1, Th17 and pathogenic Th17 (pTh17) cell-polarizing conditions by flow cytometry. Heatmap showing row-normalized geometric MFIs of the activation markers; means of 3 mice. **(L)** Representative proliferation analysis of WT and ACLY-deficient Th1 and Th17 cells by cell trace violet dilution over 4 days *in vitro*. **(M)** Representative intracellular analyses of T-bet and RORγt transcription factor expression in WT and ACLY-deficient Th1 and Th17 cells, respectively. **(N)** Flow cytometric analysis of GM-CSF and IL-2 production by WT and ACLY-deficient Th1, Th17 and pTh17 cells after re-stimulation with PMA/Iono for 5 h; means ± SEM of 6-11 mice. **(O)** Representative histopathological examination of caudal spinal cord sections from WT and *Acly*$^{fl/fl}$*Cd4*^{Cre} mice 16 days after MOG_{35-55} immunization stained with Luxol fast blue (myelin) and Cresyl violet (nuclei). **(P)** Flow cytometric analysis of immune cell infiltration in the CNS of WT and *Acly*$^{fl/fl}$*Cd4*^{Cre} mice 16 days after immunization with MOG_{35-55}; means ± SEM of 3-6 mice per cohort. **(Q** and **R)** Flow cytometric analyses of GM-CSF expression in CD4$^+$ T cells **(Q)** and quantification of total cytokine-producing CD4$^+$ T cells **(R)** in the CNS of WT and *Acly*$^{fl/fl}$*Cd4*^{Cre} mice; means ± SEM of 3-6 mice. Statistical analyses in (B), (C), (N) and (P-R) by unpaired Student's t-tests. *, $p<0.05$; **, $p<0.01$, ***, $p<0.001$.

Figure S6. Related to Figure 6

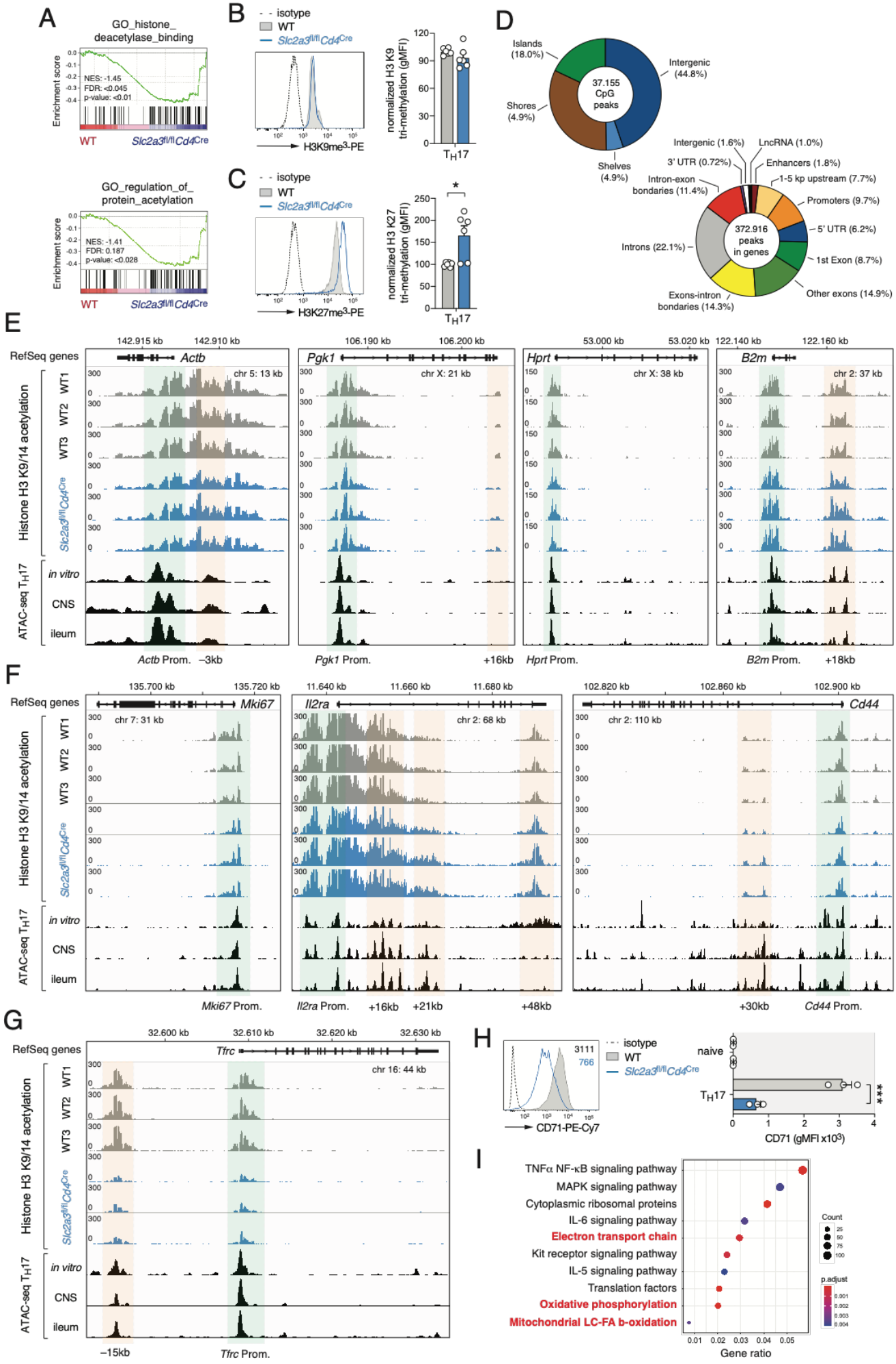

Figure S6. GLUT3-dependent acetate metabolism controls histone acetylation in Th17 cells (related to Fig. 6). **(A)** Gene set enrichment analyses (GSEA) of WT *versus* GLUT3-deficient Th17 cells indicate dysregulated protein and histone acetylation processes. **(B** and **C).** Analysis of global histone 3 (H3) tri-methylation (me^3) at lysins K9 **(B)** and K27 **(C)** in WT and GLUT3-deficient (*Slc2a3*$^{fl/fl}$*Cd4*^{Cre}) Th17 cells using flow cytometry; means ± SEM of 5-6 mice. **(D-G)** Genome-wide analysis of H3 K9/14 acetylation in WT and GLUT3-deficient Th17 cells by chromatin immunoprecipitation followed by DNA-sequencing (ChIP-seq). **(D)** Mapping of differentially acetylated regions to CpG-rich elements (upper panel) and gene bodies (lower panel) using deepTools. **(E-G)** Analysis of H3 K9/14 acetylation at housekeeping (*Actb, Pgk1, Hprt, B2m*), activation marker (*Mki67, Il2ra, Cd44*) and transferrin receptor (*Tfrc*) gene loci in WT and GLUT3-deficient Th17 cells. Promoters (green shading), enhancers and other conserved noncoding regions (orange shading) were determined using ATAC-seq datasets of different Th17 cell populations (Qiu et al., 2020). **(H)** Flow cytometric analysis of CD71 protein expression (encoded by *Tfrc*) in WT and GLUT3-deficient Th17 cells; means ± SEM of 3 mice. **(I)** Pathway enrichment analysis using differentially acetylated genes ($p < 0.05$) between WT and GLUT3- deficient Th17 cells; dot size and color represent enrichment and significance, respectively. Statistical analyses in (C) and (H) by unpaired Student's t-tests. *, $p<0.05$; **, $p<0.01$, ***, $p<0.001$.

Figure S7. Related to Figure 7

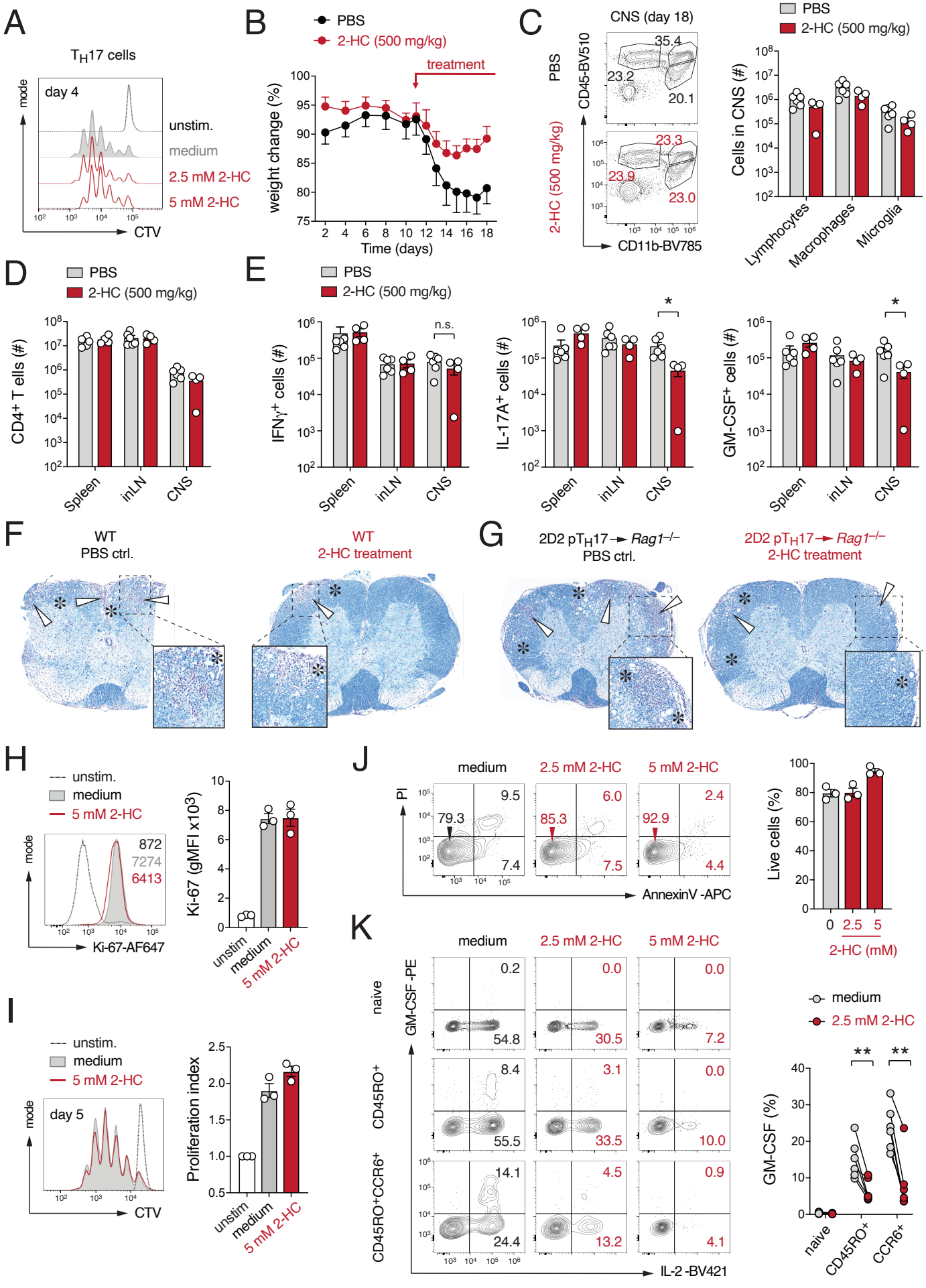

Figure S7. Pharmacological inhibition of ACLY prevents Th17 cell-mediated autoimmunity (related to Fig. 7). **(A)** Representative proliferation analysis of WT Th17 cells treated with 2-Hydroxycitrate (2-HC) using cell trace violet. **(B-G)** Treatment of mice with 2-HC ameliorates EAE immunopathology. **(B)** Relative weight change of mice after immunization with MOG_{35-55} peptide treated with or without 500 mg/kg 2-HC; means ± SEM of 4-6 mice per cohort. **(C)** Flow cytometric analysis of absolute immune cell numbers in the CNS of WT mice after immunization with MOG_{35-55} peptide with or without 500 mg/kg 2-HC treatment; means ± SEM of 4-6 mice per cohort. **(D** and **E)** Quantification of $CD4^+$ **(D)** and cytokine-producing T cells **(E)** in the spleen, inguinal (in)LNs and CNS of WT mice after immunization with MOG_{35-55} peptide with or without 500 mg/kg 2-HC treatment; means ± SEM of 4-6 mice per cohort. **(F** and **G)** Histopathological examination of caudal spinal cord sections of WT mice 18 days after MOG_{35-55} peptide immunization **(F)** and *Rag1*$^{-/-}$ mice 14 days after transfer of 2D2 Th17 cells and MOG_{35-55} peptide immunization **(G)**. Samples were stained with Luxol fast blue (myelin) and Cresyl violet (nuclei); white arrows and asterisks indicate leukocytic infiltrates and areas of demyelination, respectively. **(H-K)** 2-HC inhibits cytokine production of human $CD4^+$ memory T cells. Treatment of human PBMCs with 5 mM 2-HC does not prevent cell cycle entry (nuclear Ki-67 expression) **(H)** and proliferation (cell trace violet dilution assay) **(I)** or promotes apoptosis (Annexin V staining) **(J)** in human $CD4^+$ T cells; means ± SEM of 5 different donors. **(K)** Flow cytometric analysis of GM-CSF and IL-2 expression in naïve, $CD45RO^+$ and $CD45RO^+CCR6^+$ memory $CD4^+$ T cell subsets from healthy human donors after stimulation with PMA/Iono for 5 h in presence or absence of 2-HC; n=6 donors. Statistical analyses in (E) and (K) by unpaired Student's t-tests. *, $p<0.05$; **, $p<0.01$, ***, $p<0.001$.

Table S1. Sequences of gRNAs for CRISPR/Cas9 genome editing (Related to STAR Methods).

Name	**gRNA-sequence**	**Oligo1**	**Oligo1**
gAcly.1	GGTACGCCTCAC GCCCAAAGGGG	CACCGGGTACGCCTCACGCCCAAAG	AAACCTTTGGGCGTGAGGCGTACCC
gAcly.2	GGGTCCCACTCAT ACCTCGGAGG	CACCGGGGTCCCACTCATACCTCGG	AAACCCGAGGTATGAGTGGGACCCC
gAcly.3	CGAGTAAAATCGG TAAACTGAGG	CACCGCGAGTAAAATCGGTAAACTG	AAACCAGTTTACCGATTTTACTCGC
gAcly.4	GTCCGCTTACGAC AGCACCATGG	CACCGGTCCGCTTACGACAGCACCA	AAACTGGTGCTGTCGTAAGCGGACC

Table S2. Mouse primer for qRT-PCR (Related to STAR Methods).

Gene name	**Forward primer**	**Reverse primer**	**Source**
mouse *Acly*	ACCCTTTCACTGGGGATCACA	GACAGGGATCAGGATTTCCTTG	This study
mouse *Slc2a1*	GAGACCAAAGCGTGGTGAGT	GAGTTCGGCTATAACACTGG	This study
mouse Slc2a3	ATCGTGGCATAGATCGGTTC	TCTCAGCAGCTCTCTGGGAT	This study
mouse *18S*	CGGCGACGACCCATTCGAAC	GAATCGAACCCTGATTCCCCGT	This study
mouse *Hif1a*	AAACTTCAGACTCTTTGCTTCG	CGGCGAGAACGAGAAGAA	This study

Table S3. Primer for ChIP-qPCR (Related to STAR Methods).

Gene name	**Forward primer**	**Reverse primer**	**Source**
Mouse *Actb prom*	TGCAAAGAAGCTGTGCTCGC	GCCGTTCCGAAAGTTGCCTT	PMID: 17218320
mouse *Il17a prom*	GCAGCAGCTTCAGATATGTCC	TGAGGTCAGCACAGAACCAC	PMID: 17218320
mouse *Il17f prom*	GGGAATCAAAGGGGGACCCTAA	AAAGCAGAACCCACACGCAGAG	PMID: 22244845
mouse *Il17* CNS2	ATGGGCCTCTCTTTCCACTGATG	GGAATTTGTGGTGGAAGGGAGTG	PMID: 22244845